Electronic Supplementary Material (ESI) for Journal of Materials Chemistry C

Electronic Supporting Information

Novel Series of Quaternary Fluoride Nanocrystals: Room-Temperature Synthesis and Down-Shifting/Up-Converting Multicolor Fluorescence

Xianghong He, Bing Yan*

Department of Chemistry, Tongji University, Siping Road 1239 Shanghai 200092, China

The solvothermal procedure of M_2NaScF_6 (M = K, Rb, Cs) nanocrystallines

M_2NaScF_6 (M = K, Rb, Cs) nanocrystallines were prepared by a modified solvothermal method. Herein took the synthesis of K_2NaScF_6 nanocrystals as an example. In a typical preparation, KOH (6.67 mmol, 0.44 g), NaOH (3.33 mmol, 0.14 g), 6.00 mL deionized water, 10.00 mL alcohol, and 16.10 g oleic acid were mixed together in a plastic beaker under stirring at room temperature, followed by the addition of 4.00 mL aqueous solution of $Sc(NO_3)_3$ (0.25 M). The mixture was stirred vigorously for 120 min. Subsequently, 0.31 g HF was slowly added into the mixture under vigorous stirring. After aging for 30 minutes at 25 °C, The resultant mixing solution was then transferred into a 50 mL Teflon-lined autoclave. The autoclave was then placed in a digital temperature-controlled oven and operated at 50-200 °C for 12 hrs and then was allowed to cool to room temperature naturally. Subsequently, the as-obtained nanocrystals were collected by centrifugation at 13,000 rpm, washed sequentially with cyclohexane, water and ethanol for several times. After drying at 50 °C under dynamic vacuum for 24 hrs, K_2NaScF_6 powder was obtained. The synthetic procedure of other Sc^{3+}-cintaining fluorides hosts kept the same as that used to prepare K_2NaScF_6 host, except that KOH was replaced by RbOH or CsOH.

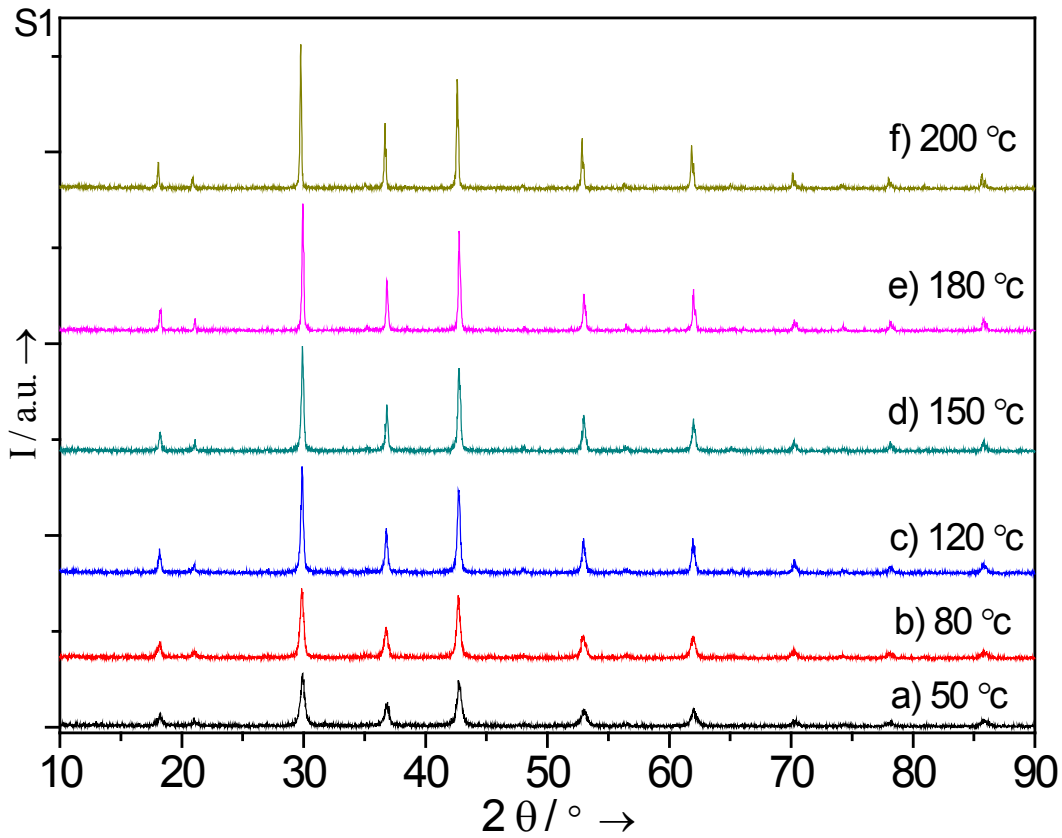

Fig. S1 XRD patterns of K_2NaScF_6 nanocrystals obtained at various temperature: a) 50, b) 80, c) 120, d) 150, e) 180, f) 200 °C.

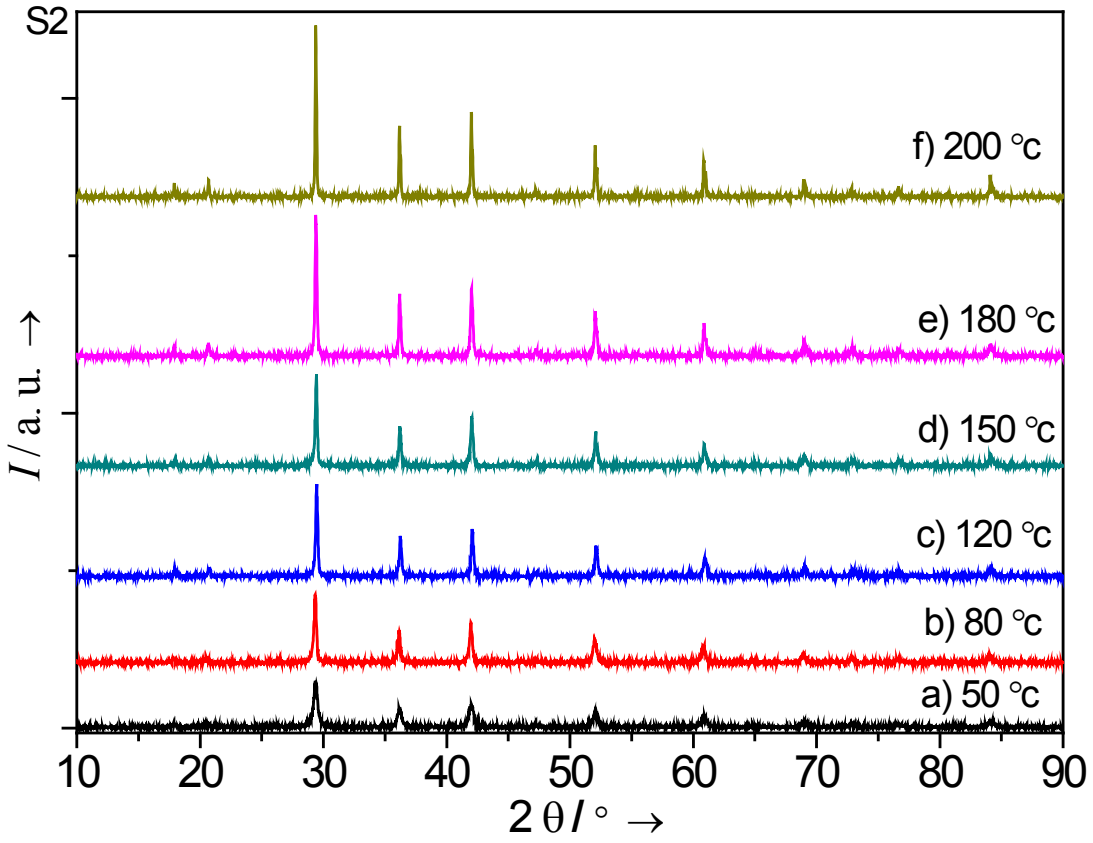

Fig. S2 XRD patterns of Rb_2NaScF_6 nanocrystals obtained at various temperature: a) 50, b) 80, c) 120, d) 150, e) 180, f) 200 °C.

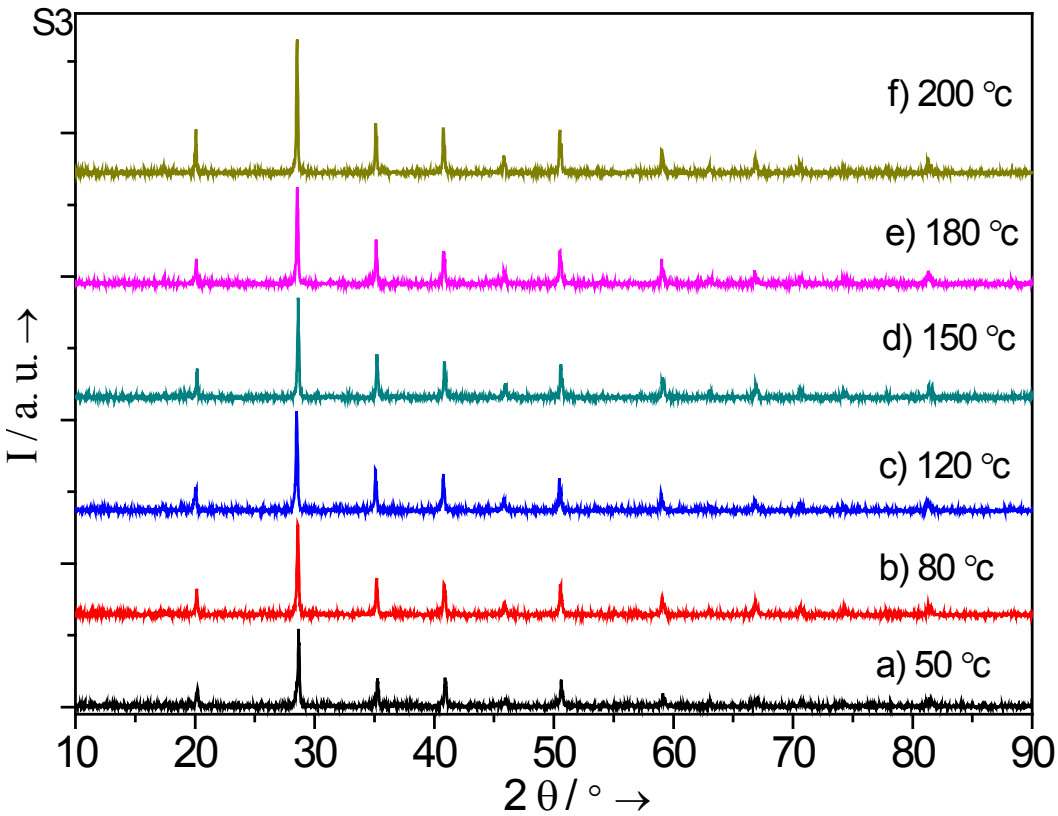

Fig. S3 XRD patterns of Cs_2NaScF_6 nanocrystals obtained at various temperature: a) 50, b) 80, c) 120, d) 150, e) 180, f) 200 °C.

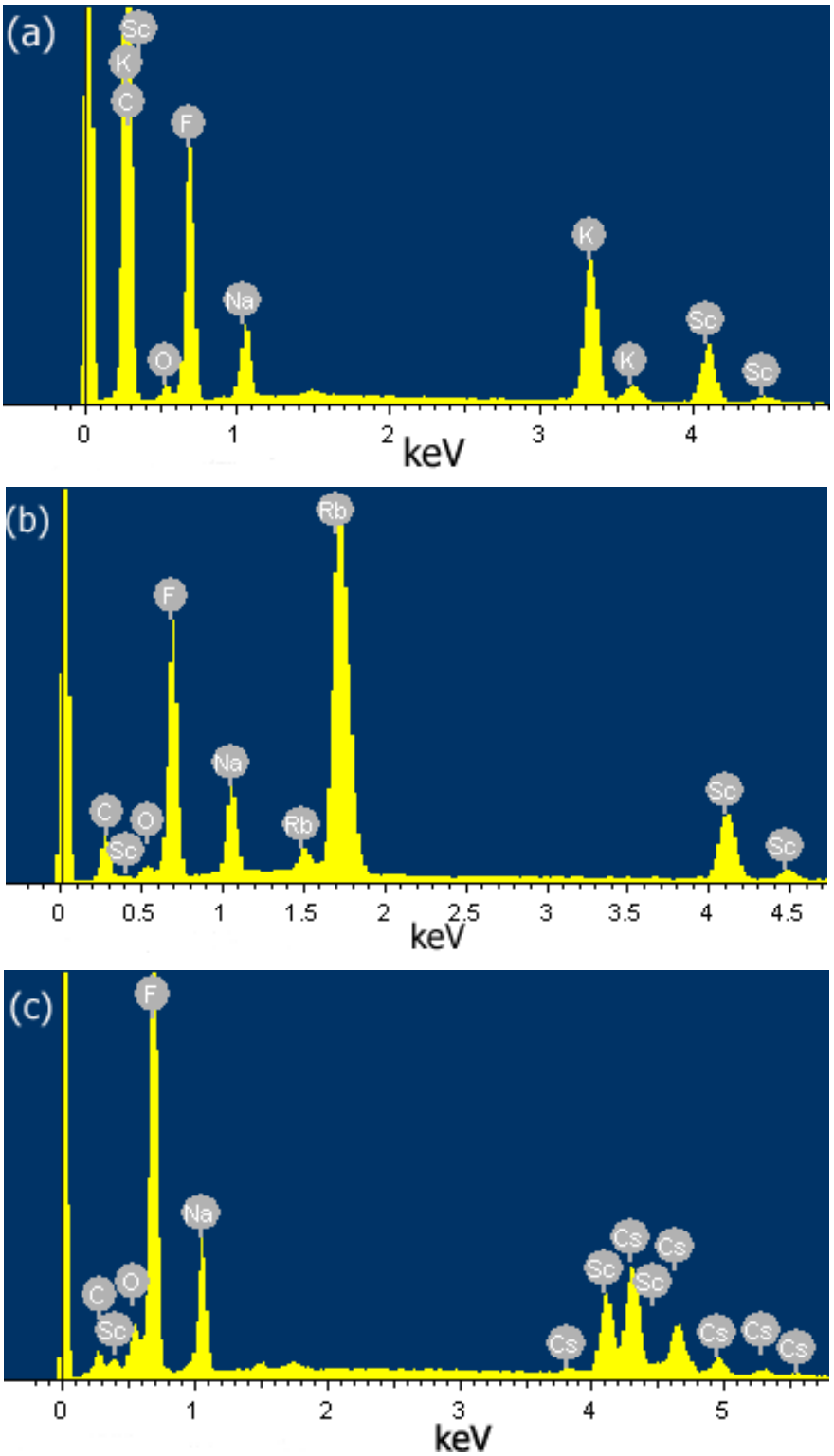

Fig. S4 EDS patterns of M_2NaScF_6 [M = (a) K, (b) Rb, (c) Cs] as-prepared nanocrystals.

Table S1 Crystal phase analysis of products under various synthetic parameters.

Synthetic conditions		Crystal phases
Without any chelator		K_2NaScF_6+ScOF+NaOH·$4H_2O$+NaOH
With OA [a]		K_2NaScF_6
With LA		K_2NaScF_6
With CA		K_2NaScF_6
Feed ratio of OA to Sc^{3+} [b]	1:1	K_2NaScF_6+ScOF+NaOH·$4H_2O$+ NaOH+NaF
	5:1	K_2NaScF_6
	10:1	K_2NaScF_6
	25:1	K_2NaScF_6
Feed ratio of (KOH+NaOH) to Sc^{3+}[c]	3:1	K_2NaScF_6+ScF_3+$KScF_4$+ KSc_2F_7+NaOH·$4H_2O$+NaF
	5:1	K_2NaScF_6
	10:1	K_2NaScF_6
	20:1	K_2NaScF_6
	30:1	K_2NaScF_6

[a] The feed ratio of OA to Sc^{3+} was 50:1, while the ratio of (NaOH+KOH)/Sc^{3+} was fixed at 10:1.

[b] The feed ratio of (NaOH+KOH)/Sc^{3+} was fixed at 10:1.

[c] The feed ratio of OA to Sc^{3+} kept at 50:1.

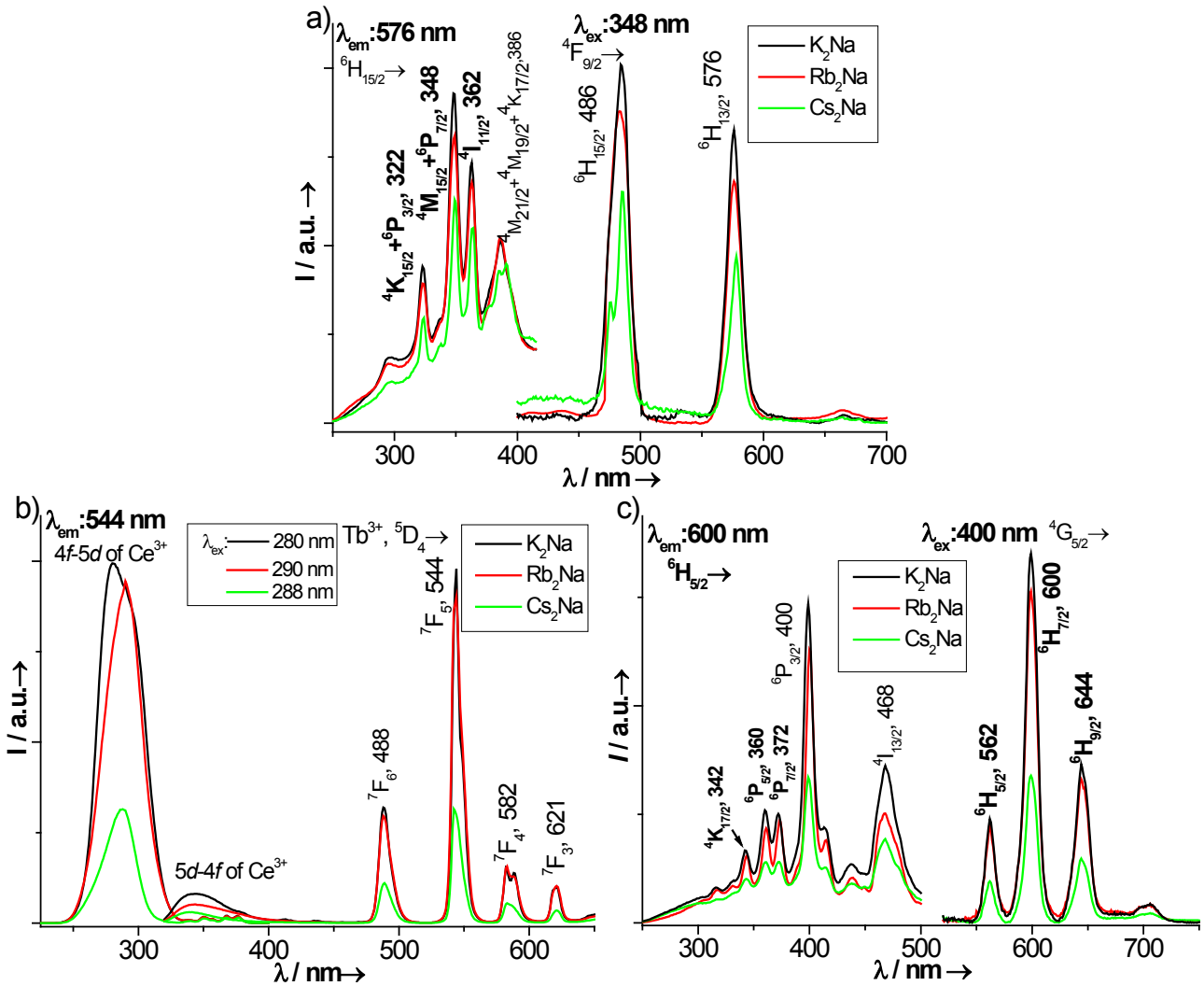

Fig. S5 DS photoluminescence excitation (left) and emission (right) spectra of $M_2NaScF_6:Ln^{3+}$ [M = K, Rb, Cs; Ln: a) Dy, b) Ce/Tb, c) Sm] nanophosphors at RT (the energy levels of excitation and emission peaks and their corresponding assignments are indicated above the curves).

Table S2 CIE chromaticity coordinates (*x*, *y*) of $M_2NaScF_6:Ln^{3+}$ (M = K, Rb, Cs; Ln = Eu, Ce/Tb, Dy, Sm) nanophosphors.

$M_2NaScF_6:Ln^{3+}$ (M = K, Rb, Cs; Ln = Eu, Ce/Tb, Dy, Sm) nanophosphors	chromaticity coordinates (*x*, *y*)
$K_2NaScF_6:Eu^{3+}$(5 mol%)	(0.5238, 0.3459)
Rb_2NaScF_6: Eu^{3+}(5 mol%)	(0.496, 0.3405)
Cs_2NaScF_6: Eu^{3+}(5 mol%)	(0.4485, 0.3262)
K_2NaScF_6: Ce^{3+}/Tb^{3+} (5 /1 mol%)	(0.3155, 0.5726)
Rb_2NaScF_6: Ce^{3+}/Tb^{3+} (5 /1 mol%)	(0.3178, 0.5817)
Cs_2NaScF_6: Ce^{3+}/Tb^{3+} (5 /1 mol%)	(0.3141, 0.5789)
$K_2NaScF_6:Dy^{3+}$(3 mol%)	(0.3043, 0.3368)
$Rb_2NaScF_6:Dy^{3+}$(3 mol%)	(0.3069, 0.3439)
$Cs_2NaScF_6:Dy^{3+}$(3 mol%)	(0.2705, 0.3066)
$K_2NaScF_6:Sm^{3+}$(3 mol%)	(0.4897, 0.3265)
$Rb_2NaScF_6:Sm^{3+}$(3 mol%)	(0.4589, 0.2863)
$Cs_2NaScF_6:Sm^{3+}$(3 mol%)	(0.4659, 0.3162)

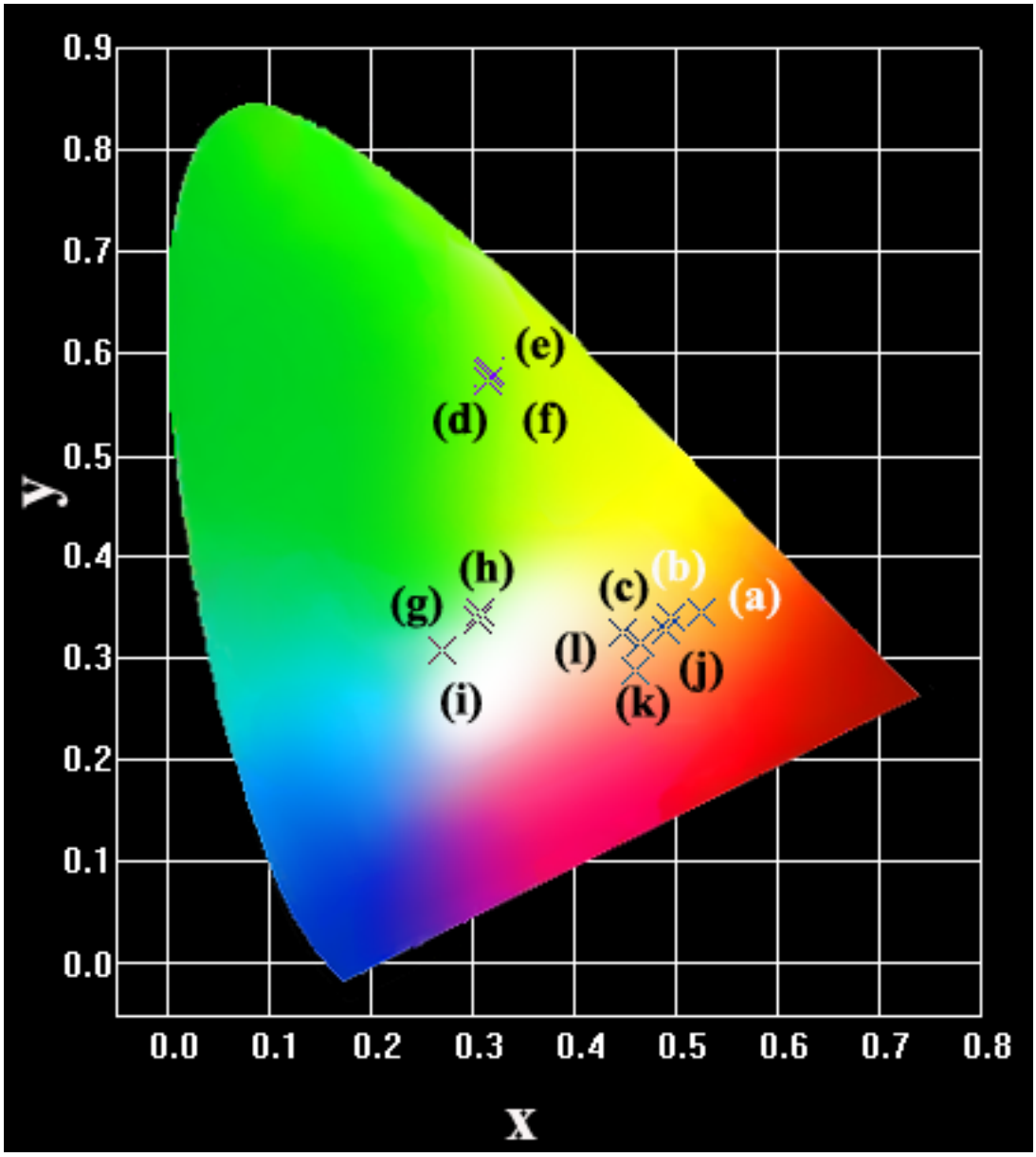

Fig. S6 CIE chromaticity diagrams for: a) K_2NaScF_6:Eu^{3+} (5 mol%), b) Rb_2NaScF_6: Eu^{3+} (5 mol%), c) Cs_2NaScF_6: Eu^{3+} (5 mol%), d) K_2NaScF_6: Ce^{3+}/Tb^{3+} (5 /1 mol%), e) Rb_2NaScF_6: Ce^{3+}/Tb^{3+} (5 /1 mol%), f) Cs_2NaScF_6: Ce^{3+}/Tb^{3+} (5 /1 mol%), g) K_2NaScF_6:Dy^{3+} (3 mol%), h) Rb_2NaScF_6:Dy^{3+} (3 mol%), i) Cs_2NaScF_6:Dy^{3+} (3 mol%), j) K_2NaScF_6:Sm^{3+} (3 mol%), k) Rb_2NaScF_6:Sm^{3+} (3 mol%), and l) Cs_2NaScF_6:Sm^{3+} (3 mol%).

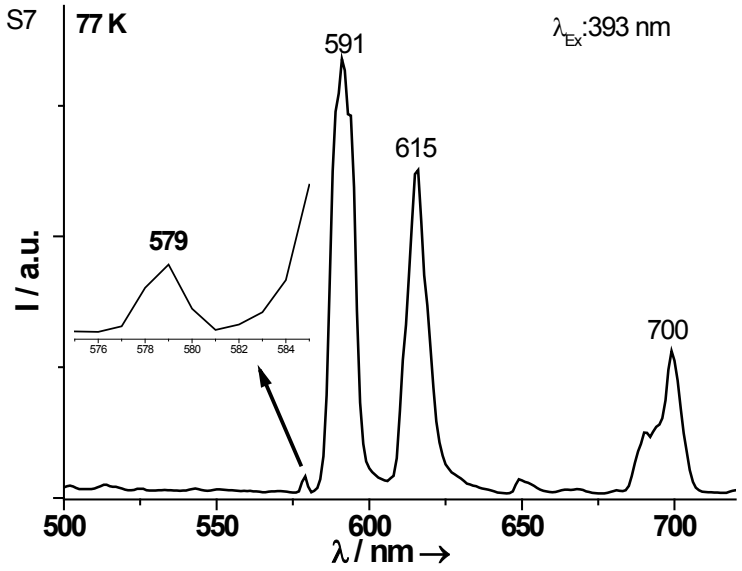

Fig. S7 DS emission spectrum at 77 K of $K_2NaScF_6:Eu^{3+}$ nanocrystals obtained at 25 °C (λ_{ex} = 393 nm, the left inset shows an expansion of the Eu^{3+} $^5D_0 \rightarrow {}^7F_0$ emission region.)

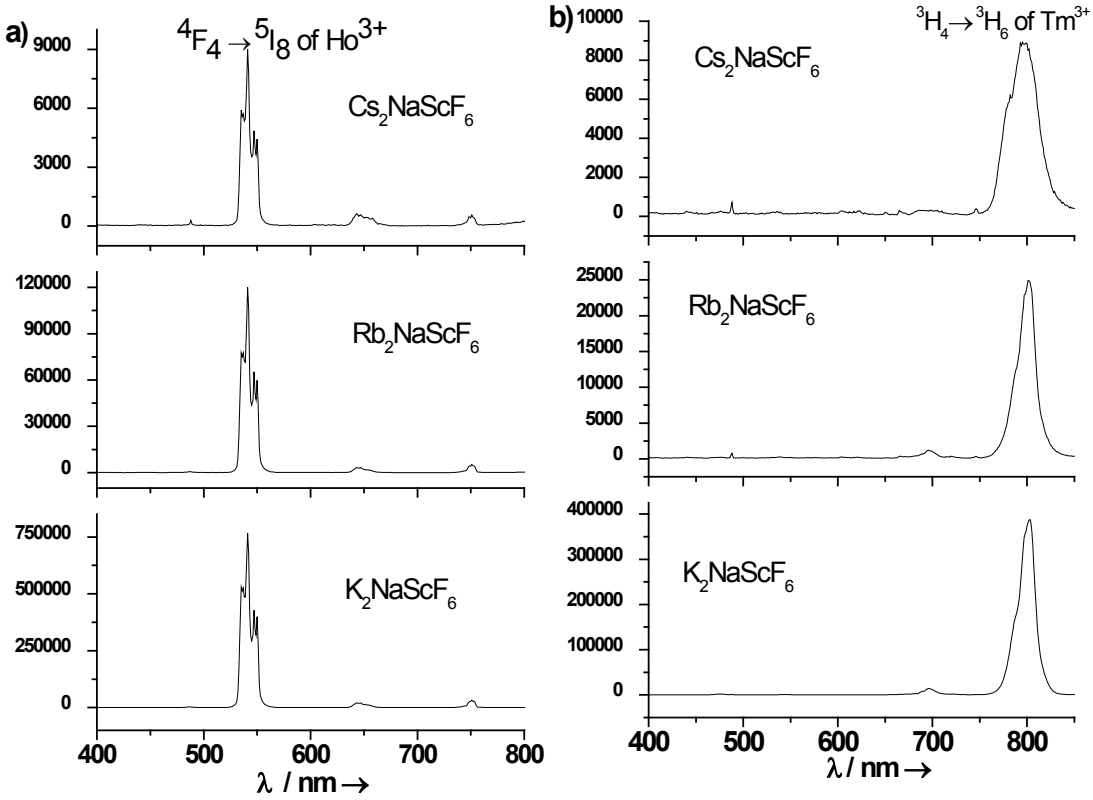

Fig. S8 UC emission spectra of : a) $(K,Rb,Cs)_2NaScF_6:Yb^{3+}/Ho^{3+}$, and b) $(K,Rb,Cs)_2NaScF_6:Yb^{3+}/Tm^{3+}$ nanocrystals (λ_{ex} = 980 nm).

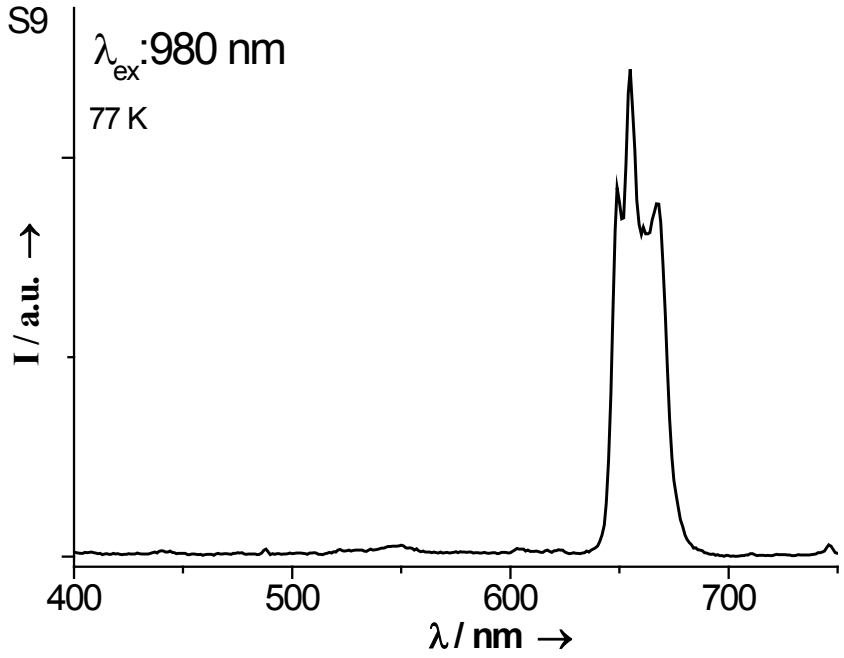

Fig. S9 UC emission spectrum at 77 K of K_2NaScF_6:Yb^{3+}/Er^{3+}(10/1 mol %) nanophosphors.

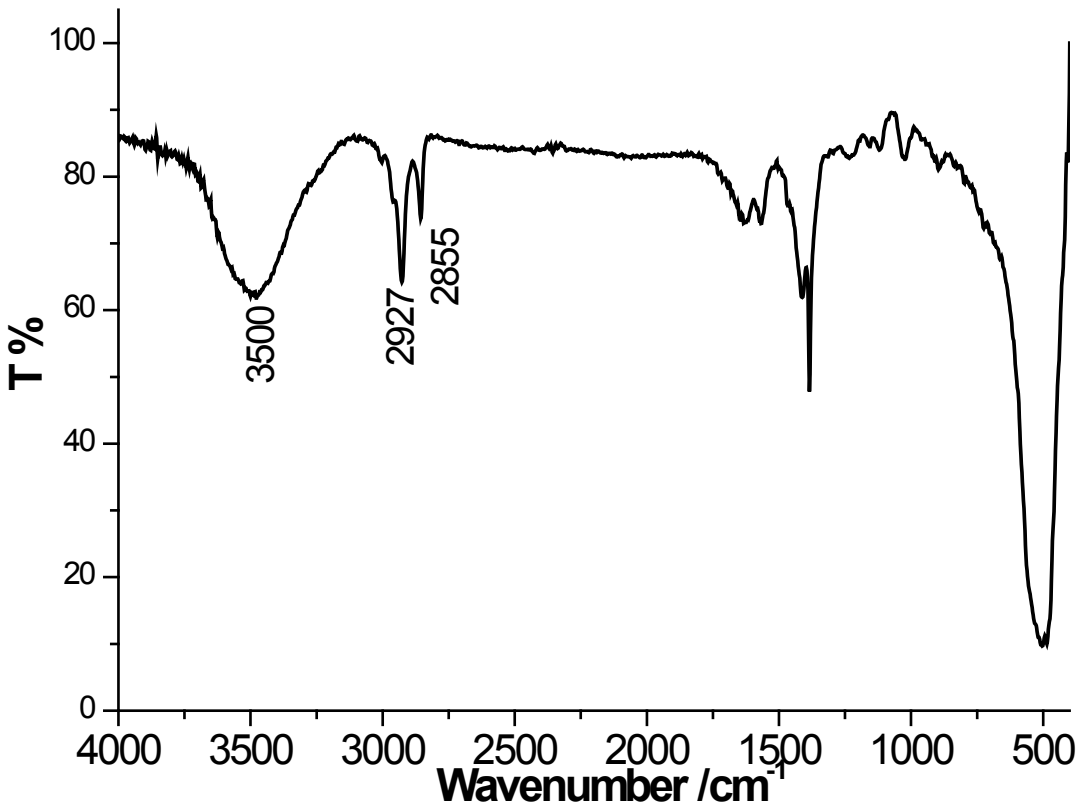

Fig. S10 Fourier transform infrared (FT-IR) spectrum of as-obtained K_2NaScF_6 NCs

Generally, there are three possible processes populating $^4F_{9/2}$ level of Er^{3+} ion resulting in red UC emission. The first one is direct population from $^4I_{13/2}$ level, which can be populated through the nonradiative relaxation of $^4I_{11/2}$ level ($^4I_{11/2} \rightarrow {}^4I_{13/2}$), and the second one is via a nonradiative relaxation from $^4S_{3/2}$ level ($^4S_{3/2} \rightarrow {}^4F_{9/2}$), while the third one is realized by a cross relaxation process ($^4F_{7/2} + {}^4I_{11/2} \rightarrow 2\ {}^4F_{9/2}$) between two adjacent Er^{3+} ions. The two former processes emphasize the importance of multiphonon relaxation. Herein, Yb^{3+}/Er^{3+} co-activated M_2NaScF_6 (M = K, Rb, Cs) nanocrystals (NCs) remained a single-band UC emission even at the low-temperature (77 K) (Fig. S9, ESI), indicating that the phonon participation in the transfer process has only a slight effect on the emission. On the other hand, Fourier transform infrared (FT-IR) spectrum of as-obtained K_2NaScF_6 indicated that the surface is capped by the organic groups (Fig. S10, ESI). Due to the presence of the organic groups on the surface of the nanoparticles, the multiphonon relaxation process is regarded as an efficient process. The organic groups including -OH, $-CH_3$, and $-CH_2$ possess high-energy vibrational modes (2800-3600 cm^{-1}), in comparison with the dominant phonon modes in K_2NaScF_6 (236 cm^{-1}). These high energy vibrations would strongly quench the excited states of Er^{3+} ions by multiphonon relaxation and thus influence the upconversion processes significantly. The gap energy between $^4I_{11/2}$ and $^4I_{13/2}$ states and between $^4S_{3/2}$ and $^4F_{9/2}$ states is around 3600, and 3000 cm^{-1}, respectively. The high-energy vibrations from -OH, $-CH_3$, and $-CH_2$ organic groups make the multiphonon relaxation ($^4I_{11/2} \rightarrow {}^4I_{13/2}$ and $^4S_{3/2} \rightarrow {}^4F_{9/2}$) much more probable than that of the intrinsic phonons in K_2NaScF_6 host, where at least thirteen phonons are required to bridge these gaps. Therefore, we speculated that the almost banned green emission is related to the larger population of $^4F_{9/2}$ level of Er^{3+} ions via multiphonon relaxation in the presence of high-energy vibrational organic groups on the surfaces of NCs.

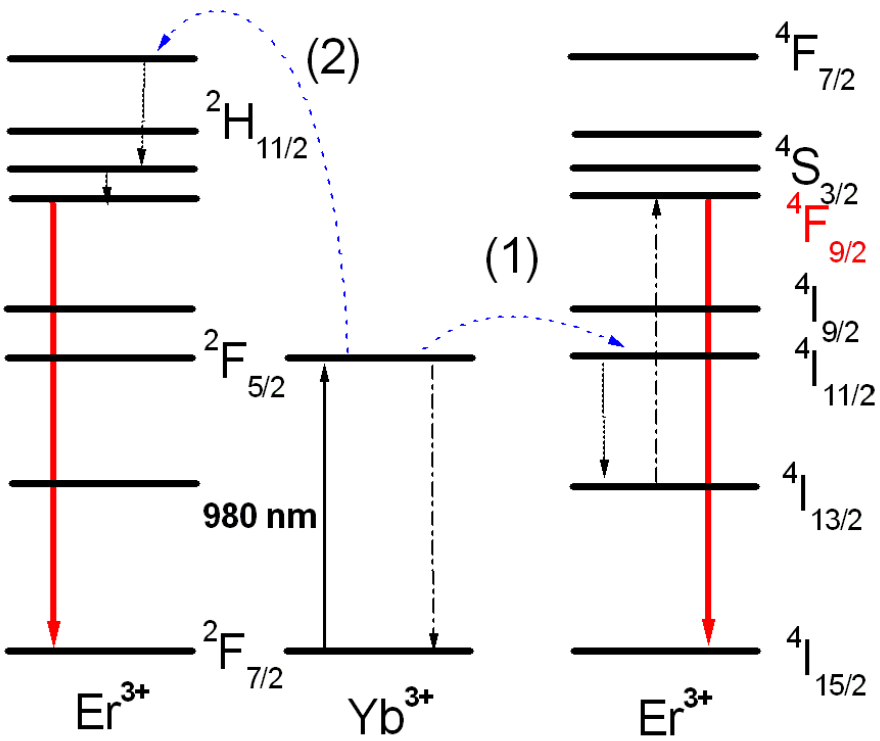

Fig. S11 Schematic energy level diagram, and up-converting red emission scheme for $K_2NaScF_6:Yb^{3+}/Er^{3+}$(10/1 mol %) nanophosphors [process (1) is direct population from $^4I_{13/2}$ level, which is populated through the nonradiative relaxation of $^4I_{11/2}$ level ($^4I_{11/2} \rightarrow {}^4I_{13/2}$), and process (2) is via a nonradiative relaxation from $^4S_{3/2}$ level ($^4S_{3/2} \rightarrow {}^4F_{9/2}$)].